PHOTOPRODUCTION OF η-MESONS AND $\eta\pi$-PAIRS OFF LIGHT NUCLEI *

B. Krusche

Department of Physics, University of Basel, Switzerland

(Received January 7, 2014)

Photoproduction of η-mesons has been measured for several light nuclei (^{2}H, ^{3}He, ^{7}Li) and photoproduction of $\eta\pi$-pairs was investigated for a deuteron target. The experiments were done at the tagged photon beam of the Mainz MAMI accelerator with the Crystal Ball/TAPS electromagnetic calorimeter. They aimed at two topics: the extraction of cross section data for the elementary reactions off neutrons and the investigation of the η-nucleus interactions, in view of η-mesic states. The main results are: the excitation function for the $\gamma n \to n\eta$ reaction has a very narrow structure (width around 30 MeV) at final state invariant masses of 1670 MeV. Its nature is not yet understood. For the quasi-free production of $\eta\pi$-pairs, the analysis of all isospin channels (final states $p\eta\pi^0$, $n\eta\pi^0$, $p\eta\pi^-$, and $n\eta\pi^+$) resulted in cross section ratios almost perfectly agreeing in the threshold region with a dominant contribution from the $D_{33} \to \eta P_{33}(1232) \to \eta\pi N$ decay chain. The measurement of coherent η-production off ^{3}He and ^{7}Li nuclei confirmed a strong threshold enhancement accompanied by almost isotropic angular distributions for the ^{3}He nucleus and much smaller deviations from PWIA approximations for the ^{7}Li nucleus, supporting the special role of ^{3}He as a candidate for η-mesic nucleus formation.

DOI:10.5506/APhysPolB.45.639
PACS numbers: 13.60.Le, 14.20.Gk, 14.40.Aq, 25.20.Lj

1. Introduction

Photoproduction of mesons off light nuclei is an important tool for two different lines of research [1]. It is the only practical approach for the investigation of the elementary reactions off (quasi-free) neutrons and it can shed light on meson–nucleus interactions, in particular on the conjectured formation of mesic nuclei, *i.e.* quasi-bound states of mesons in nuclei generated by the strong interaction.

* Presented at the II International Symposium on Mesic Nuclei, Kraków, Poland, September 22–25, 2013.

Both topics have been investigated with quasi-free and coherent photoproduction of mesons off light nuclei at the MAMI accelerator in Mainz with the Crystal Ball/TAPS experiment. Here, we report the most recent experimental results for the photoproduction of η-mesons and $\eta\pi$-pairs.

The isospin structure of electromagnetic nucleon-resonance excitations can only be revealed by the comparison of meson production reactions off the proton to the corresponding reactions off the neutron. Since free neutrons are not available, it is unavoidable to extract the information about the elementary $\gamma n \rightarrow Nx$ reactions (N — nucleon, x — any meson or mesons) from experiments using nuclear targets. Compared to the free $\gamma p \rightarrow Nx$ reactions, measured with hydrogen targets, several complications must be overcome. The simpler ones are of technical nature, arising from the coincident detection of the recoil nucleons necessary to identify the initial state of the reaction and to reconstruct completely the reaction kinematics so that the effects of nuclear Fermi motion can be eliminated. More problematic are nuclear effects summarized as the final state interactions (FSI) such as nucleon–nucleon or nucleon–meson rescattering, which can modify reaction probabilities, angular distributions *etc.* of the elementary reactions off the free nucleon for nucleons embedded in a nucleus. Due to these complications, the experimental program to study meson production reactions off the neutron is still much less developed than the corresponding program for the free proton, where in addition to total cross sections, angular distributions, and single polarization observables already first results for double polarization observables become available.

The technical problems have been basically solved, modern detection systems like the electromagnetic calorimeters used for the present experiments, can efficiently identify the recoil nucleons. The measurement of their polar and azimuthal angles with sufficient experimental resolution is straightforward in highly segmented detectors. The measurement of kinetic energies is most of the time only possible for recoil protons. Recoil neutrons do not deposit well defined amounts of energy that could be related to their initial kinetic energy, and time-of-flight paths are usually too short to extract the kinetic energy from timing measurements. However, when deuterons are used as target nuclei, the measurement of the momenta (and masses) of the mesons and the angles of the recoil nucleons is already sufficient. The kinetic energy of the recoil nucleon can then be reconstructed from energy and momentum conservation [1]. In this way, the effects from nuclear Fermi motion can be very efficiently eliminated. The nuclear FSI effects, on the other hand, cannot be eliminated. Here we have three different options. We can use models that try to reproduce and predict such effects, we can in the case of the proton compare the results for measurements off the free proton to the results for protons bound in nuclei (and try to understand this way under which conditions and for which reaction channels such effects are important), and we can compare experimental results for different light nuclei. Examples for such strategies are the cross sections measurements of η- [2, 3] and η'-production [4] off the neutron and the measurement of beam-helicity asymmetries for π^0-pairs off the neutron [5], for which the comparison of free and quasi-free proton cross sections suggested that nuclear effects are negligible. A completely different case is single pion production in the nucleon resonance region, where very significant nuclear effects have been observed for the $\gamma d \to pp\pi^-$ reaction [6] as well as for the $\gamma d \to np\pi^0$ reaction [7].

While on the one hand, FSI effects represent an obstacle for the investigation of the meson production reactions off neutrons, they offer on the other hand a unique chance to study meson–nucleus interactions. For long-lived mesons, like charged pions or kaons, secondary beams can be used for detailed studies of elastic and inelastic reactions, revealing the relevant potentials. However, most mesons are short-lived so that their interaction with nucleons can only be studied in indirect ways, making use of the final-state interactions (FSI). The general idea is to produce the mesons with some initial reaction in a nucleus and then study their interaction with the same nucleus. A very interesting, controversially discussed topic is, whether quasi-bound states can be formed between nuclei and mesons. Such states would be an ideal laboratory for the study of the properties of the strong interaction in view of meson–nucleus dynamics. The interaction of low-energy pions with nucleons is much too weak for the formation of bound states, but the situation is different for η and possibly also for η' mesons.

Photoproduction of η-mesons off the nucleon in the threshold region is characterized by the strong contribution of the excitation of the s-wave $S_{11}(1535)$ nucleon resonance [8], which has an $\approx 50\%$ branching ratio to $N\eta$ [9]. As a consequence, the ηN interaction at low η-momentum is strong. Measurements of η-photoproduction off light to heavy nuclei [10, 11] have revealed a scaling of the production cross section proportional to $A^{1/3}$ ($A =$ nuclear mass number), indicating strong absorption corresponding to an elementary ηN reaction cross section around 30 mb and a mean free path of ≈ 2 fm. Based on the approximation of the ηN scattering length, Liu and Haider [12] suggested already more than 25 years ago the possible existence of quasi-bound η-nucleus systems for medium-light nuclei like carbon and oxygen. More recently, following more precise input data for the scattering length, interest focused on light nuclei like the helium isotopes. Studied was, in particular, the threshold behaviour of η-production reactions with hadronic and electromagnetic probes. Among the possible signatures for quasi-bound states, there are threshold enhancements of the production reactions. The most promising signals have so far been found for the ^{3}He nucleus, with hadron- [13–17] as well as with photon-induced [18, 19] reactions. Here, we will summarize the most recent results from photoproduction for ^{3}He and ^{7}Li nuclei and future perspectives for the ^{4}He nucleus.

2. Experimental setup

The experiments were done at the Mainz MAMI accelerator [20], delivering primary electron beams of ≈ 1.5 GeV. Bremsstrahlung photons were produced in thin radiator foils (typically 10 μm copper) and tagged with the upgraded Glasgow magnetic spectrometer [21]. The typical bin width of the photon beam energy is defined by the geometrical size of the plastic scintillators in the focal plane detector of the tagger. The intrinsic resolution of the magnetic spectrometer is better by more than an order of magnitude. Liquid cryo-targets were used for the measurements with deuterium and helium, and a solid target was used for lithium. The helium target cell (cylindrical shape, 3 cm diameter, 5.08 cm length, surface density 0.073 nuclei/barn) was made from mylar, the target cells for the deuterium were Kapton cylinders (4 cm and 3 cm diameter, respectively 4.72 cm length, surface densities 0.147, 0.231 nuclei/barn). The solid ^{7}Li target was 5.4 cm long (surface density 0.264 nuclei/barn). Contributions from the mylar and Kapton cells were determined with empty target measurements.

A schematic representation of the detector setup is shown in Fig. 1. It combined the electromagnetic calorimeters Crystal Ball (CB) [22] and TAPS [23]. The CB, made of 672 NaI crystals covered the full azimuthal range for polar angles from 20° to 160°, corresponding to 93% of the full solid angle. The TAPS detector was configured as a forward wall combining 384 hexagonally shaped BaF_2 crystals which was placed 1.457 m downstream from the target and covered polar angles between $\approx 5°$ and 21°.

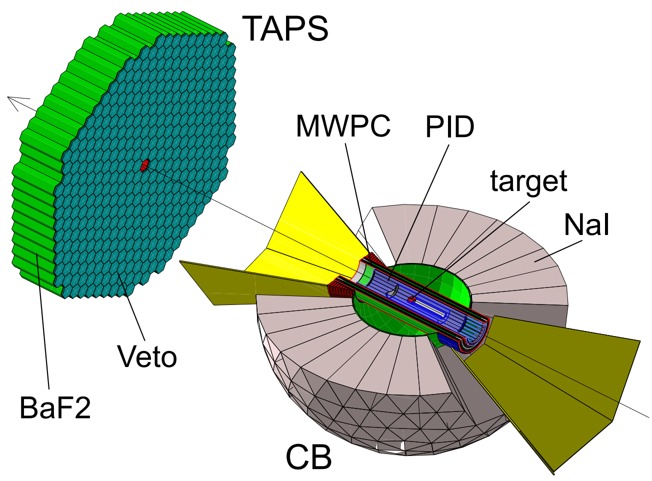

Fig. 1. Experimental setup combining Crystal Barrel (CB, only lower half shown), TAPS, and charged-particle identification detectors. Target in the center of the CB, beam from the lower-right to upper-left corner.

The Crystal Ball was equipped with an additional Particle Identification Detector (PID) for the identification of charged particles and all modules of the TAPS detector had individual plastic scintillators (CPV) in front for the same purpose.

The trigger conditions were different for the different targets (because apart from η-production the runs combined data taking for several other reaction channels). The main trigger components were always a condition for the analog energy sum of all modules of the CB and conditions on the multiplicity of hits in the complete calorimeter.

3. Data analysis

The data analysis procedures are described in detail in [19, 24, 25]. The main steps for all data start with the classification of calorimeter hits as 'charged' or 'neutral' using the PID and the TAPS CPV. Subsequently, the pulse-shape analysis for the BaF_2 modules and a time-of-flight *versus* energy analysis complete the identification of photons, neutrons, and protons in TAPS. A ΔE–E analysis with PID and CB was used for the identification of protons and charged pions in the CB. Separation of photons and neutrons was not directly possible for hits in the CB. Therefore, for events with an odd number of neutral hits, and no positive identification of a neutral hit in TAPS as neutron, all neutral hits in the CB were treated as photon and neutron candidates and the most probable assignment was done with a χ^2 analysis of the invariant masses of photon pairs (for the hypotheses of π^0- or η-decays). Different event classes were analyzed for the investigated reactions. All quasi-free production reactions were analyzed in coincidence with recoil protons, recoil neutrons, and inclusively (*i.e.* without any condition for recoil nucleons). Quasi-free η-production was analyzed for the $\eta \rightarrow 2\gamma$ and $\eta \rightarrow 3\pi^0 \rightarrow 6\gamma$ decays. Thus events with two neutral, three neutral, two neutral plus one charged, six neutral, seven neutral, and six neutral plus one charged hit were analyzed. Coherent η-production was analyzed under the condition that no recoil nucleon was observed, *i.e.* only events with exactly two or six neutrals were accepted. The identification of the mesons was done with standard invariant mass analyses. The separation of quasi-free and coherent η-production was based on missing mass analyses, which were also used to eliminate background from $\pi\eta$-pairs (when the pion had escaped from detection).

4. Elementary reactions off nucleons

4.1. Photoproduction off η-mesons

Tremendous progress has been made in the study of photoproduction of η-mesons off protons. Apart from the pion, this is now probably the best studied final state. Total cross sections and angular distributions have been measured at all major tagged photon facilities even with repeated and improved experiments [26–36]. Also some results for single polarization observables have been published [31, 37–39] and with electroproduction experiments a large range of Q^2 has been explored [40–42]. The current experimental status for photoproduction is summarized in Fig. 2. Shown are the total cross section and the coefficients of a fit of Legendre polynomials to the angular distributions

$$\frac{d\sigma}{d\Omega} = \sum_{i=0}^{4} A_i P_i \left(\cos\left(\Theta_\eta^\star\right)\right) , \qquad (1)$$

where $\Theta_\eta^\star$ is the η cm polar angle. The results have been normalized to the A_0 coefficient, which is proportional to the total cross section.

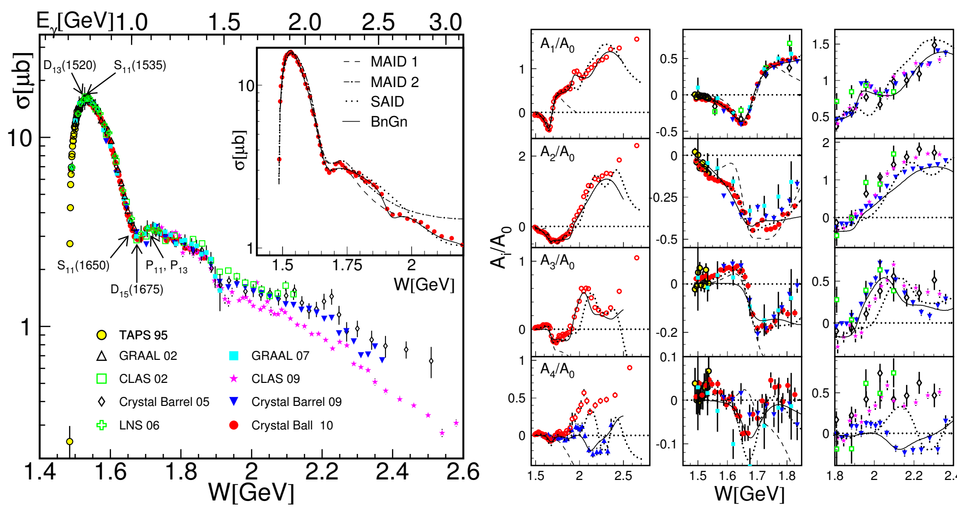

Fig. 2. Left-hand side: total cross section data of the $\gamma p \to p\eta$ reaction (extracted from fits of the angular distributions). Data from [26] (TAPS 95), [27] (GRAAL 02), [28] (CLAS 02), [29] (Crystal Barrel 05), [30] (LNS 06), [31] (GRAAL 07), [33] (Crystal Barrel 09), [34] (CLAS 09), [36] (Crystal Ball 10). Model curves from [43] (MAID 1), [44] (MAID 2), [45] (BnGn), [46] (SAID). Right-hand side: Legendre coefficients of the angular distributions. Left column: full energy range, average over all data except for A_4, for which the data from [33] is shown separately. Central (right) column: individual data sets for low (high) energy range.

The data from the different measurements are in fairly good agreement. The absolute normalization of the CLAS 09 data [34] differs at large excitation energies from the other data sets (note that after normalization to A_0 the Legendre coefficients agree with the other data sets). The A_4 coefficient for the Crystal Barrel 09 data [33] deviates from all other data sets. However, these data are the only ones which cover the extreme forward angles to which the A_4 coefficient is very sensitive.

All models agree on the strong dominance of the $S_{11}(1535)$ resonance in the threshold region and a destructive interference between this state and the $S_{11}(1650)$. A tiny contribution from the $D_{13}(1525)$ resonance was identified in the angular distributions [26] and, in particular, in the photon-beam asymmetry Σ [37, 39]. The corresponding decay branching ratio of this state into $N\eta$ is very small, it amounts only to $(0.23 \pm 0.04\%)$ [9].

The reaction is much less understood at little higher incident photon energies. The results from different models do not agree among each other (compare, for example, the model results for the total cross section in the insert at the left-hand side of Fig. 2). Even worse, different analyses suggest different contributions of nucleon resonances. As discussed in [39], in the BnGn analysis [45] the $P_{11}(1710)$ makes an almost negligible contribution while the $P_{13}(1720)$ is essential to describe the beam asymmetries. On the other hand, in the 'Eta-MAID' model [43] the P_{11} is more important than the P_{13}. The shape of the angular distributions changes dramatically for meson–nucleon invariant masses W between 1.6 and 1.7 GeV (see Fig. 2, right-hand side, central column).

Quasi-free and coherent photoproduction of η-mesons off light nuclei (^{2}H [47–50], ^{4}He [51, 52]) was in the past mainly studied in the threshold region and used to extract the isospin structure of the electromagnetic excitation of the $S_{11}(1535)$ resonance. The main result (see Ref. [53] for a summary) was that the excitation is dominantly of isovector nature with an $A^{\mathrm{IS}}_{1/2}/A^{p}_{1/2} = 0.09 \pm 0.01$ ratio, where $A^{p}_{1/2}$ is the helicity-1/2 coupling for the proton and $A^{\mathrm{IS}}_{1/2}$ its isoscalar component. At higher incident photon energies, models [43] predicted a much larger contribution of the $D_{15}(1675)$ state in the neutral channel, so that the neutron/proton cross section ratio should rise. However, the experimental finding [2, 3, 54] was a pronounced structure in the $n\eta$-excitation function in the W range, where the angular distributions for the $\gamma p \rightarrow p\eta$ undergo the rapid change. The nature of this structure is not yet understood, different scenarios have been discussed including interferences between the excitations of known nucleon resonances [55, 56], coupled channel effects [57, 58], threshold effects from opening strangeness production [59] but also intrinsically narrow excited nucleon states [55, 60–62].

The existence of this structure has recently been confirmed with two high statistics experiments done at the MAMI accelerator using liquid deuterium and liquid ^{3}He targets [25, 63]. Total cross sections as function of final state invariant mass W are summarized in Fig. 3. The invariant mass W was extracted as discussed in [1, 3] so that the effects from nuclear Fermi

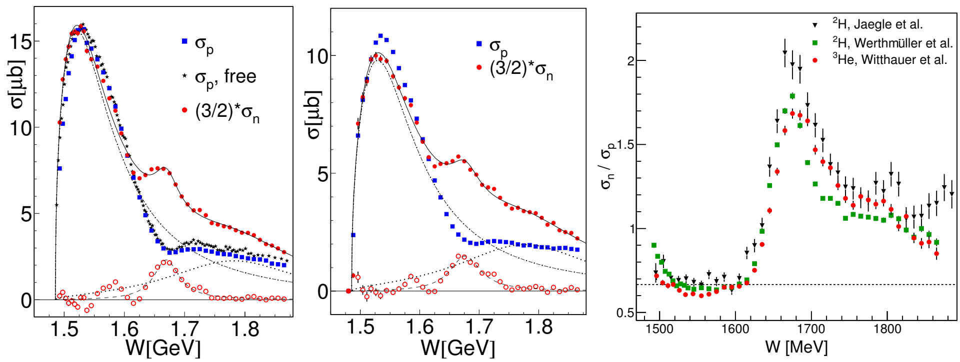

Fig. 3. Quasi-free excitation functions for $\gamma N \to N\eta$. Left-hand side: deuteron [63] and free proton [36] targets; quasi-free proton (squares/blue), free proton (stars/black), and quasi-free neutron (circles/red). Curves: fits (see the text): S_{11} contribution (dash-dotted), phenomenological background (dotted), narrow structure (dashed), sum of all (solid). Open circles/red: data after subtraction of S_{11} and background fit. Center: same for ^{3}He target [25, 63]. Right-hand side: ratio of neutron/proton excitation functions [3, 25, 63].

motion were removed. The results for the quasi-free reaction off protons bound in the deuteron [63] are in excellent agreement with free proton data [36]. This demonstrates the quality of the kinematical reconstruction of the Fermi motion effects and suggests that re-scattering and other FSI effects are not important. The data have been fitted with a phenomenological ansatz adding three Breit–Wigner (BW) curves, one for the dominant $S_{11}(1535)$ contribution, one to parameterize other background contributions, and one to parameterize the narrow structure. The results for the ^{3}He target show the same structure, although the effects from Fermi smearing are, of course, much more important. The only difference is that the quasi-free cross sections from the ^{3}He target are smaller by about 25% than free proton or quasi-free deuteron data. Thus FSI effects for the ^{3}He target are not negligible, but do not seem to influence the narrow structure, which appears very stable independent of the nuclear environment. We thus conclude that this structure is indeed a genuine feature of the free $\gamma n \to n\eta$ reaction. From the fits, a most probable position of $W = (1670 \pm 5)$ MeV and a width of $\Gamma = (30 \pm 15)$ MeV were extracted. When treated like an s-wave resonance, the corresponding coupling strength $\sqrt{b_\eta}A^n_{1/2}$ is approximately $(12.3 \pm 0.8) \times 10^{-3}$ GeV$^{-1/2}$. Precise angular distributions extracted from these experiments are currently under analysis in the framework of reaction models. Data for the target asymmetry T and the double polarization observables E and F have already been measured and are under analysis.

4.2. Photoproduction of $\eta\pi$-pairs

Photoproduction of meson pairs should give access to excited nucleon states which have no significant decay branching ratios directly to the nucleon ground state but decay preferentially via cascades involving intermediate excited states. Such behaviour is, in particular, probable for high lying states in the excitation range of the 'missing' nucleon resonances. The best studied double-meson final state are pion pairs. In particular, double π^0 production has been studied (see *e.g.* [5, 64, 65]) which has the advantage that due to the small coupling of photons to neutral pions, non-resonant background contributions are suppressed.

More recently also the $\eta\pi$ final state attracted much interest. Total cross sections, invariant mass distributions, and also some polarization observables have been measured for the $\gamma p \to p\pi^0\eta$ reaction [30, 66–72] This decay channel is very selective. The η-meson is isoscalar, so that nucleon resonances can only emit it in $N^\star \to N^{(\star)}$ or $\Delta^\star \to \Delta^{(\star)}$ transitions. The analysis of the available data [68, 71] suggested a dominant contribution from the $D_{33}(1700) \to \eta P_{33}(1232) \to \eta\pi N$ cascade in the threshold region.

As discussed below, in that case, the reaction would be very interesting for the search for η-mesic nuclei because one can expect a significant contribution from coherent production for target nuclei (*e.g.* ^{4}He) for which coherent single η-production is strictly forbidden.

When the reaction is indeed dominated by the $D_{33} \to \eta P_{33} \to \eta\pi N$ cascade, simple predictions can be made for the cross section ratios of the different charge states. The electromagnetic helicity couplings for the excitation of Δ resonances are identical for protons and neutrons, and from the Clebsch–Gordon coefficients of the different hadronic decays one arrives immediately at

$$\sigma\left(\gamma p \to \eta\pi^0 p\right) = \sigma\left(\gamma n \to \eta\pi^0 n\right) = 2\sigma\left(\gamma p \to \eta\pi^+ n\right) = 2\sigma\left(\gamma n \to \eta\pi^- p\right) , \tag{2}$$

while for the photoexcitation of an $N^\star$ resonance the factors 2 would be 1/2 and the cross section ratios for neutron and proton targets could be anything. Data for all four isospin channels has been measured recently at MAMI. Preliminary results for total cross sections and their ratios are summarized in Fig. 4. They are in excellent agreement with the above expectations for the $D_{33} \to \eta P_{33} \to \eta\pi N$ cascade. The absolute scale of the cross sections for the quasi-free proton bound in the deuteron are suppressed with respect to the free proton by roughly 25%–30%, so that significant FSI effects are observed.

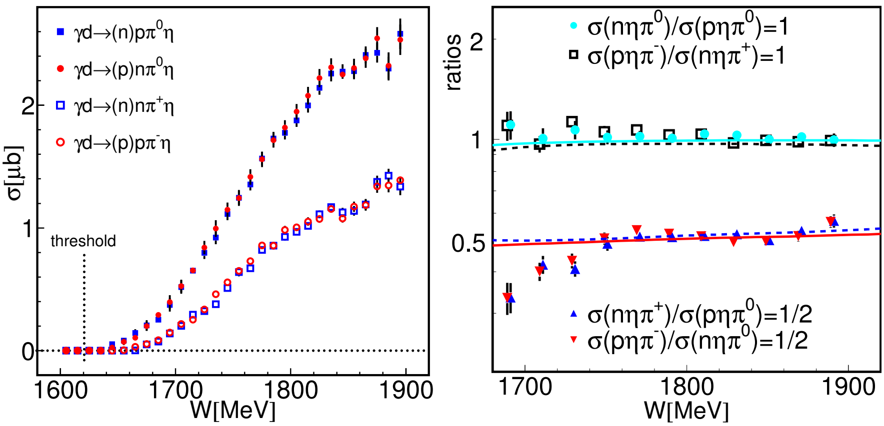

Fig. 4. Quasi-free excitation functions for $\gamma N \rightarrow N\eta\pi$ measured with a deuteron target. Left-hand side: total cross sections, right-hand side: cross section ratios. All data preliminary. Model curves from [71, 73].

5. Coherent production off η-mesons off ^{3}He and ^{7}Li nuclei

The threshold behaviour of meson production reactions can give important clues for the formation of quasi-bound states. The idea is that strongly attractive meson–nucleus interactions will give rise to threshold enhancements of the production cross section independent of the initial state. The threshold behaviour of many hadron induced reactions like $pp \rightarrow pp\eta$ [74–76], $np \rightarrow d\eta$ [77, 78], $pd \rightarrow \eta^3$He [13], $dp \rightarrow \eta^3$He [14, 15, 17], $dd \rightarrow \eta^4$He [79], $\vec{d}d \rightarrow \eta^4$He [80, 81], and $pd \rightarrow pd\eta$ [82] has been studied. Interesting effects have been found for most of them, but, in particular, the $pd \rightarrow \eta^3$He [13] and $dp \rightarrow \eta^3$He reactions [14, 15, 17] show an extremely steep rise at threshold. And there are also indications [16] that not only the magnitude but also the phase of the s-wave amplitude of this reaction varies rapidly in the threshold region.

When these threshold effects are due to strong FSI, they should also appear in photon induced reactions, which motivated the study of the threshold behaviour of photoproduction off η-mesons off light nuclei. The difficulty for such experiments is that on the one hand breakup reactions, where nucleons are removed from the incident nucleus, are difficult to interpret because the final nuclear state is not known and on the other hand, coherent production is strongly suppressed by the nuclear form factors and for many nuclei completely forbidden due to the relevant quantum numbers. As discussed in Sec. 4.1, η-threshold production is dominated by an isovector, spin-flip transition. Consequently, only nuclei with spin $J \neq 0$ and isospin $I \neq 0$ are promising candidates. For light, stable nuclei, ^{3}He and ^{7}Li fulfil this condition. The first observation of coherent η-production for the ^{3}He nucleus was reported in [18]. A strong threshold enhancement was indeed found, although the statistical quality of the data was limited and the separation of coherent events and incoherent background was difficult, so that ambiguities about the exact threshold behaviour persisted.

Recently, the ^{3}He measurement was repeated at the MAMI accelerator with the CB/TAPS experiment [19], covering almost the full solid angle. This improved not only the statistical quality of the results, but helped also for the separation of coherent and breakup reactions (the separation is done by missing mass analysis, but for an almost 4π covering detector a significant fraction of the breakup background is already suppressed due to the detection of the recoil nucleons). An ^{7}Li target was studied with the same experimental setup. The measured total cross sections are summarized in Fig. 5 and compared to simple plane-wave-impulse approximations (PWIA).

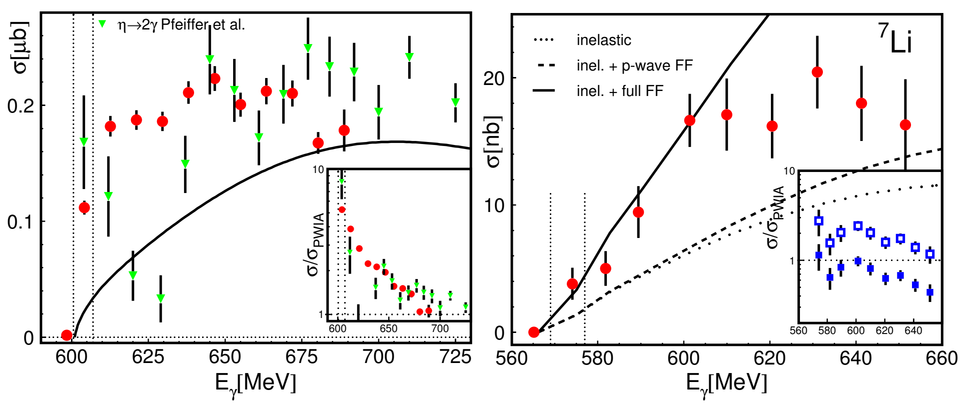

Fig. 5. Total cross section for the $\gamma^3\text{He} \to \eta^3\text{He}$ [19] (left-hand side) and the $\gamma^7\text{Li} \to \eta^7\text{Li}$ [24] (right-hand side) coherent η-production reactions. The light grey/green triangles for ^{3}He are from [18]. The curves are from PWIA modelling. For the Li-target, the inelastic contribution (excitation of low lying nuclear state) is shown separately and calculations using the full elastic form factor or only the p-wave part are shown. The dotted lines indicate coherent and breakup thresholds. The inserts show the ratio of data and PWIA prediction, for Li for the full and p-wave form factor.

The extremely steep rise of the cross section for ^{3}He nuclei could be confirmed. The somewhat strange dip structure reported from the previous ^{3}He experiment could be ruled out as an statistical artefact resulting from the unfavourable signal-to-background ratio in that energy range. On an absolute scale, the cross section for the ^{7}Li target is roughly smaller by an order of magnitude. This is more or less reproduced by the PWIA modelling and related to the nuclear form factor. Here, one should note that the coherent

η-production behaves much different than for example coherent π^0-production in the Δ resonance region. In the latter case, going from ^{3}He to ^{7}Li, one looses also an order of magnitude in scale due to the form factor, but one regains a factor of 5.5 from the A^2-term (A = nuclear mass number) in the PWIA. Since the η-production is so strongly dominated by an isovector spin-flip, in ^{3}He only the odd $s_{1/2}$ neutron and in ^{7}Li only the odd $p_{3/2}$ proton contributes, so that the A^2 factor from the coherent addition of the amplitudes from all nucleons is lost.

The comparison of the total cross sections to the PWIA modelling highlights the special role of the ^{3}He–η system. The rise at threshold is much steeper than expected from PWIA. Also the behaviour of the angular distributions [19], which are almost isotropic or even slightly backward enhanced at threshold, is different from PWIA behaviour, where they are forward peaked due to the form factor influence. On the other hand, the behaviour of the ^{7}Li–η system is much more like expected from PWIA. There is no abrupt rise at threshold, and the angular distributions [24] are forward peaked.

6. Conclusions and outlook

The photoproduction of η-mesons and $\eta\pi$-pairs has been studied with the CB/TAPS experiment at MAMI for several light nuclei. The measurements off the deuteron were motivated as a study of the elementary reactions off the neutron, and are part of a larger program running at MAMI and ELSA, covering different final states and more recently also polarization observables. Among the most interesting results, there is a pronounced narrow structure in the excitation function of the $\gamma n \rightarrow n\eta$ reaction which has also been confirmed in a measurement using a ^{3}He target. The nature of this structure is not yet understood and new data for the polarization observables T, E, and F will further constrain reaction models, which so far can describe the structure with different scenarios.

Quasi-free production of $\eta\pi$-pairs has been studied for all possible final states $p\pi^0\eta$, $n\pi^0\eta$, $n\pi^+\eta$, and $p\pi^-\eta$ off the deuteron. The experimentally found cross section ratios are almost in perfect agreement with the expectation (see Eq. (2)) for a dominant contribution from a $\Delta^\star \rightarrow \eta\Delta \rightarrow \eta\pi N$ cascade.

In terms of FSI effects, single η-production and the production of $\eta\pi$-pairs behaves differently. For single η-production, no significant nuclear effect is observed, the quasi-free production cross section for protons bound in the deuteron agrees with the cross section measured for the free proton. For $\eta\pi$-pairs a suppression of the order of 30% is observed for production off quasi-free protons compared to the free proton. For η-production a suppression of roughly 25% of quasi-free production off nucleons bound in ^{3}He compared to free protons or quasi-free nucleons bound in the deuteron is observed. The analysis of the quasi-free reactions off ^{3}He nuclei is still under way.

The study of coherent η-production off ^{3}He and ^{7}Li nuclei has underlined the special role of the ^{3}He–η system. A very strong threshold enhancement combined with isotropic or even backward enhanced angular distributions has been observed for this nucleus, confirming its role as so far best candidate for an η-mesic state. The behaviour of the ^{7}Li–η system is much less spectacular and can be fairly well reproduced with PWIA modelling.

For the future, it is planned to measure quasi-free and coherent photoproduction of $\pi^0\eta$-pairs of ^{4}He. This is the only promising way to search for ^{4}He η-mesic states in photoproduction reactions since due to its quantum numbers coherent single η-photoproduction off ^{4}He nuclei is forbidden, but based on the strong dominance of the $\Delta^\star \rightarrow \eta\Delta \rightarrow \eta\pi N$ cascade in the threshold region the coherent production of $\eta\pi$-pairs is not forbidden and kinematics can be selected such that the pion takes away the momentum and the η has a very small momentum relative to the nucleus.

The results summarized in this work are part of the experimental program of the A2 Collaboration at MAMI and have been obtained by the Ph.D. works of A. Käser, Y. Maghrbi, F. Pheron, D. Werthmüller, and L. Witthauer. This work was supported by Schweizerischer Nationalfonds (200020-132799,121781,117601,113511), Deutsche Forschungsgemeinschaft (SFB 443, SFB/TR 16), DFG-RFBR (Grant No. 05-02-04014), the UK Science and Technology Facilities Council, (STFC 57071/1, 50727/1), European Community-Research Infrastructure Activity (FP6), the US DOE, US NSF and NSERC (Canada).

REFERENCES

[1] B. Krusche, *Eur. Phys. J. Special Topics* **198**, 199 (2011).
[2] I. Jaegle *et al.*, *Phys. Rev. Lett.* **100**, 252002 (2008).
[3] I. Jaegle *et al.*, *Eur. Phys. J.* **A47**, 89 (2011).
[4] I. Jaegle *et al.*, *Eur. Phys. J.* **A47**, 11 (2011).
[5] M. Oberle *et al.*, *Phys. Lett.* **B721**, 237 (2013).
[6] V.E. Tarasov *et al.*, *Phys. Rev.* **C84**, 035203 (2011).
[7] M. Dieterle *et al.*, submitted to *Phys. Rev. Lett.*
[8] B. Krusche *et al.*, *Phys. Lett.* **B397**, 171 (1997).
[9] M. Beringer *et al.*, *Phys. Rev.* **D86**, 010001 (2012).
[10] M. Röbig-Landau *et al.*, *Phys. Lett.* **B373**, 45 (1996).

[11] T. Mertens *et al.*, *Eur. Phys. J.* **A38**, 195 (2008).
[12] L.C. Liu, Q. Haider, *Phys. Rev.* **C34**, 1845 (1986).
[13] B. Mayer *et al.*, *Phys. Rev.* **C53**, 2068 (1996).
[14] J. Smyrski *et al.*, *Phys. Lett.* **B649**, 258 (2007).
[15] T. Mersmann *et al.*, *Phys. Rev. Lett.* **98**, 242301 (2007).
[16] C. Wilkin *et al.*, *Phys. Lett.* **B654**, 92 (2007).
[17] T. Rausmann *et al.*, *Phys. Rev.* **C80**, 017001 (2009).
[18] M. Pfeiffer *et al.*, *Phys. Rev. Lett.* **92**, 252001 (2004).
[19] F. Pheron *et al.*, *Phys. Lett.* **B709**, 21 (2012).
[20] K.-H. Kaiser *et al.*, *Nucl. Instrum. Methods* **A593**, 159 (2008).
[21] J.C. McGeorge *et al.*, *Eur. Phys. J.* **A37**, 129 (2008).
[22] M. Oreglia *et al.*, *Phys. Rev.* **D25**, 2259 (1982).
[23] A.R. Gabler *et al.*, *Nucl. Instrum. Methods* **A346**, 168 (1994).
[24] Y. Maghrbi *et al.*, *Eur. Phys. J.* **A49**, 38 (2013).
[25] L. Witthauer *et al.*, *Eur. Phys. J.* **A49**, 154 (2013).
[26] B. Krusche *et al.*, *Phys. Rev. Lett.* **74**, 3736 (1995).
[27] F. Renard *et al.*, *Phys. Lett.* **B528**, 215 (2002).
[28] M. Dugger *et al.*, *Phys. Rev. Lett.* **89**, 222002 (2002).
[29] V. Crede *et al.*, *Phys. Rev. Lett.* **94**, 012004 (2005).
[30] T. Nakabayashi *et al.*, *Phys. Rev.* **C74**, 035202 (2006).
[31] O. Bartalini *et al.*, *Eur. Phys. J.* **A33**, 169 (2007).
[32] O. Bartholomy *et al.*, *Eur. Phys. J.* **A33**, 133 (2007).
[33] V. Crede *et al.*, *Phys. Rev.* **C80**, 055202 (2009).
[34] M. Williams *et al.*, *Phys. Rev.* **C80**, 045213 (2009).
[35] M. Sumihama *et al.*, *Phys. Rev.* **C80**, 052201(R) (2009).
[36] E.F. McNicoll *et al.*, *Phys. Rev.* **C82**, 035208 (2010).
[37] J. Ajaka *et al.*, *Phys. Rev. Lett.* **81**, 1797 (1998).
[38] A. Bock *et al.*, *Phys. Rev. Lett.* **81**, 534 (1998).
[39] D. Elsner *et al.*, *Eur. Phys. J.* **A33**, 147 (2007).
[40] C.S. Armstrong *et al.*, *Phys. Rev.* **D60**, 052004 (1999).
[41] R. Thompson *et al.*, *Phys. Rev. Lett.* **86**, 1702 (2001).
[42] H. Denizli *et al.*, *Phys. Rev.* **C76**, 015204 (2007).
[43] W.-T. Chiang *et al.*, *Nucl. Phys.* **A700**, 429 (2002).
[44] W.-T. Chiang *et al.*, *Phys. Rev.* **C68**, 045202 (2003).
[45] V.A. Anisovich *et al.*, *Eur. Phys. J.* **A25**, 427 (2005).
[46] R.A. Arndt *et al.*, `http://gwdac.phys.gwu.edu`
[47] B. Krusche *et al.*, *Phys. Lett.* **B358**, 40 (1995).
[48] P. Hoffmann-Rothe *et al.*, *Phys. Rev. Lett.* **78**, 4697 (1997).

[49] J. Weiss *et al.*, *Eur. Phys. J.* **A11**, 371 (2001).
[50] J. Weiss *et al.*, *Eur. Phys. J.* **A16**, 275 (2003).
[51] V. Hejny *et al.*, *Eur. Phys. J.* **A6**, 83 (1999).
[52] V. Hejny *et al.*, *Eur. Phys. J.* **A13**, 493 (2002).
[53] B. Krusche, S. Schadmand, *Prog. Part. Nucl. Phys.* **51**, 399 (2003).
[54] V. Kuznetsov *et al.*, *Phys. Lett.* **B647**, 23 (2007).
[55] V.A. Anisovich *et al.*, *Eur. Phys. J.* **A41**, 13 (2009).
[56] A.V. Anisovich *et al.*, *Eur. Phys. J.* **A49**, 67 (2013).
[57] V. Shklyar, H. Lenske, U. Mosel, *Phys. Lett.* **B650**, 172 (2007).
[58] R. Shyam, O. Scholten, *Phys. Rev.* **C78**, 065201 (2008).
[59] M. Döring, K. Nakayama, *Phys. Lett.* **B683**, 145 (2010).
[60] R.A. Arndt *et al.*, *Phys Rev.* **C69**, 035208 (2004).
[61] A. Fix, L. Tiator, M.V. Polyakov, *Eur. Phys. J.* **A32**, 311 (2007).
[62] M. Shrestha, D.M. Manley, *Phys. Rev.* **C86**, 055203 (2012).
[63] D. Werthmüller *et al.*, *Phys. Rev. Lett.* **111**, 232001 (2013).
[64] U. Thoma *et al.*, *Phys. Lett.* **B659**, 87 (2008).
[65] A.V. Sarantsev *et al.*, *Phys. Lett.* **B659**, 94 (2008).
[66] J. Ajaka *et al.*, *Phys. Rev. Lett.* **100**, 052003 (2008).
[67] I. Horn *et al.*, *Phys. Rev. Lett* **101**, 202002 (2008).
[68] I. Horn *et al.*, *Eur. Phys. J.* **A38**, 173 (2008).
[69] E. Gutz *et al.*, *Eur. Phys. J.* **A35**, 291 (2008).
[70] E. Gutz *et al.*, *Phys. Lett.* **B687**, 11 (2010).
[71] V. Kashevarov *et al.*, *Eur. Phys. J.* **A42**, 141 (2009).
[72] V. Kashevarov *et al.*, *Phys. Lett.* **B693**, 551 (2010).
[73] A. Fix, private communication.
[74] H. Calén *et al.*, *Phys. Lett.* **B366**, 39 (1996).
[75] J. Smyrski *et al.*, *Phys. Lett.* **B474**, 182 (2000).
[76] P. Moskal *et al.*, *Phys. Rev.* **C69**, 025203 (2004).
[77] F. Plouin, P. Fleury, C. Wilkin, *Phys. Rev. Lett.* **65**, 690 (1990).
[78] H. Calén *et al.*, *Phys. Rev. Lett.* **80**, 2069 (1998).
[79] A. Wronska *et al.*, *Eur. Phys. J.* **A26**, 421 (2005).
[80] N. Willis *et al.*, *Phys. Lett.* **B406**, 14 (1997).
[81] A. Budzanowski *et al.*, *Nucl. Phys.* **A821**, 193 (2009).
[82] F. Hibou *et al.*, *Eur. Phys. J.* **A7**, 537 (2000).